# Discrete Element Modeling of 3D Irregularly-Shaped Particles

M. M. Mollanouri, A. A. Mirghasemi
*School of Civil Engineering, College of Engineering, University of Tehran, Tehran, Iran*

2011 Pan-Am CGS Geotechnical Conference

ABSTRACT
To model the behaviour of granular materials, it's very ideal that granular particles being simulated the same as real ones in the nature. The method that is employed in this paper is in fact a more similar modeling of grain's shape to the reality. In this way, the real shape of grain is modeled by combining arbitrary number of overlapping spheres, which are connected to each other in a rigid way. A program that is based on Discrete Element Method (DEM) has been developed which makes necessary changes to accommodate real grain shape rather than the traditional spherical modeling. In the purpose of comparing the effects of grains shape on mechanical behavior of granular soils, three types of grains, high angular, medium angular, and round grains are modeled. Several triaxial tests are performed on assemblies with different grain types. The results demonstrate that the angularity of grains is considerably affecting the behavior of soil.

RÉSUMÉ
Pour modeler l'agissement des matérieux granuleux, c'est très idéal de simuler les particules granuleuses comme leurs formes reélles, existées dans la nature. En effet la méthode employée dans cet article c'est le modelage plus réel de la forme de la graine. Dans cette façon la forme réelle de la graine an été modelée par la combinaison d'un nombre arbitraire des éléments sphériques qui ont des liens et qui se joignent rigidement. Alors un programme a été écrit, basé sur la méthode des éléments discrets (MED) qui fait des changements necessaires pour préparer la forme réelle de la graine au lieu du modelage sphérique traditionnel. Trois types de la graine, aïgu, moyen et rond, ont été modélés pour comparer les effets des formes des graines sur l'agissement mécanique des sols granuleux. Ensuite plusieurs analyses tièdres réalisent sur l'assemblage de chaque type de la graine. Les resultants démontrent que les angles superficiels des graines influencent considérablement sur l'agissement mécanique du sol.

## 1 INTRODUCTION

Initially, Cundall and Struck (1979) developed discrete element method (DEM). This method considers assembly of distinct particles interacting by means of contact forces. In a given system every particle can move transitionally and rotationally. Over 30 years, developments in DEM have made it possible to model variety of physical phenomena in the nature. These improvements expand the utilization of DEM in many areas such as physics and chemistry. Most 2D and 3D DEM simulations have used disks and spherical particles. In this method, contact between grains can be detected with simple algorithms; furthermore, disks and spherical grains can move easily in each other's neighborhood. But distinct particles happen to have various shapes in reality; therefore, modeling with disks and spheres cannot be highly accurate. For example, the internal friction angle of shearing resistance and the resistance to rotation for spherical grains is much less than that of actual ones. Moreover, the direction of the contact normal forces is always toward the center in spherical modeling, and this leads to the idea that these forces never contribute to moments acting on the grains; therefore, rotation is only affected by the contact tangential forces.

As a result, different methods for modeling non-spherical and non-circular particles such as ellipsoids and ellipse-shaped grains (Rothenburg & Bathurst 1992, Ting, Khawaja et al. 1993, Ng 1994 and Lin & Ng, 1997; Ouadfel and Rothenburg, 1999; Bagherzadeh- Khalkhali & Mirghasemi 2009), polyhedral and polygon-shaped particles, (Hart, Cundall et al., 1988; Barbosa & Ghaboussi 1992, Mirghasemi et al 1997, 2002; Xu, C., Zhu, J., 2006; Seyedi Hosseininia & Mirghasemi 2006, 2007, and Bagherzadeh-Khalkhali et al 2008), have been presented to be used in DEM modeling in order to improve the result of simulations. Furthermore, M. Kodam at el (2009) in their research mentioned that many non-spherical particle shape have been suggested such as superquadrics (Williams and Pent- land, 1992; Hogue, 1998; Cleary andSawley,2002), sphero-cylinders (Abreu etal.,2003; Langston et al.,2004), and arbitrary shapes using discrete function representations (Hogue and Newland,1994; Williams and O'Connor,1995); Perhaps, the most commonly used non-spherical particle shape algorithm is the glue-sphere method (Gallas and Sokolowski, 1993; Haff, 1993; Ristow, 1994; Nolan and Kavanagh, 1995; Abou-Chakra etal., 2004). Nearly, in all methods mentioned above, the direct modeling of grain's shape is not considered. Matsushima and Saomoto (2002) proposed a direct modeling method of irregularly-shaped granular materials and showed its high adaptability to 2-D and 3-D DEMs.

For sure, particle shape has a significant effect on the behavior of granular materials. Many researchers have experienced this phenomenon (Roberts and Beddow, 1968/69; Aoki and Suzuki, 1971); because of the significant effects of grain's shape on mechanical behavior of soils; it seems praiseworthy to conduct

discrete element modeling with grains whose shapes are exactly modeled.

In this paper, a collection of irregularly-shaped granular particles are generated, and then triaxial tests are conducted on the generated assemblies. Finally, the influence of angularity on mechanical behaviour of granular material with different confining stress and friction coefficients are investigated.

## 2 MODELING OF REAL PARTICLE SHAPE

Matsushima & Saomoto (2002), Matsushima et al. (2003) used a simple algorithm in 2D and 3D to find the optimized number of circular and spherical elements, respectively, to model real shape of grain as shown in Figure 1.

The procedure of particle modeling consists of three steps. At first, particles with different angularities are considered. Then, they are smoothed to prepare a particle that can fill with some spheres. Finally, they are replaced with combined spheres. It can be seen that created shape with these spherical elements, is very similar to real (initial) shape of the grain.

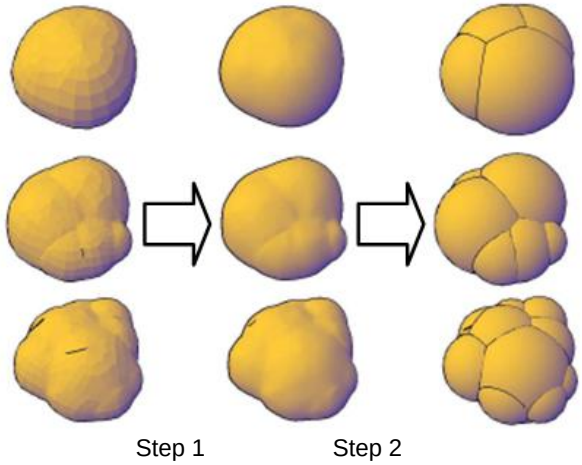


Figure 1. Three steps for modeling real shape particles with different angularities by sphere elements

As presented a single particle with different angularities is modeled above. The number of sphere elements for modeling grain's shape depends on the degree of non-uniformity and angularity of actual grain's shape, the desired level of accuracy for grain's shape and limitation that is considered for computation time.

This method, when real shape of particles is modeled, can be used to gain more realistic results for mechanical behaviour of granular soils. Therefore, the results of simulated assemblies of grains can be compared with experimental results of actual assemblies.

The program TRUBAL (Cundall and Strack 1979) was adopted and modified to simulate assembly of particles which are represented according to above assumption. In the developed program, the contact considerations and calculations of contact forces are conducted for each sphere element of grain and the equation of motion is solved for each grain. As a result, it allows sphere elements of each grain join together in a rigid way. Furthermore, contact detection is changed for finding contact between real shape particles.

## 3 THREE ANGULARITY CATEGORIES

To investigate the effects of different shapes of grains on mechanical behaviour of granular materials, three series of grains with different angularity were considered: high angular grains, medium angular grains and rounded grains. In the first step, 5 types of high angular grains were chosen with equivalent diameter ranged from 10mm to 40mm. Then, medium angular grains and round grains were generated through reduction of angularity in high angular grains. In other words, general shape and size of each grain's type was similar for three series as shown in Figure 2.

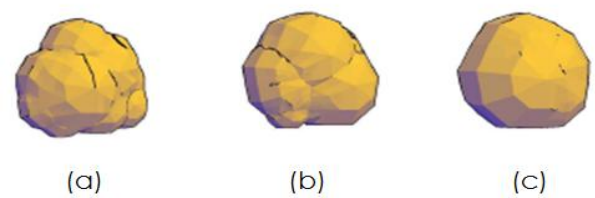


Figure 2. (a) High angular grain, (b) Medium angular grain, (c) Rounded grain

The results of researches show that grains eccentricity has considerable effects on mechanical behaviour. Therefore, in order to consider only the effects of angularity on behaviour, eccentricity was eliminated; In other words, it was tried to surround the grains with squares instead of rectangles. In the next step, the grains were modeled by combining sphere elements as it was described in section 3.

## 4 GRAIN SHAPE PREPARATION

Five types of particles were modeled (Figure 4). Each type consists of a clump of spherical elements that the number of them depends on the grade of angularity of that type. By increasing angularity the number of spherical elements is increased. In this study 1000 grains were used for each series of assembly. The grain size distribution of the modeled grains is shown in Figure 3. In this figure, equivalent diameter is the diameter of the sphere that is circumscribed about every irregularly-shaped particle.

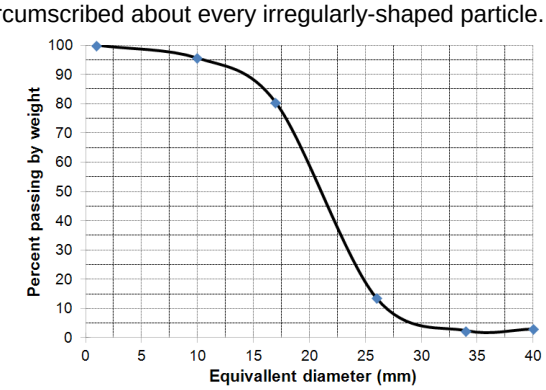

Figure 3. Grain size distribution

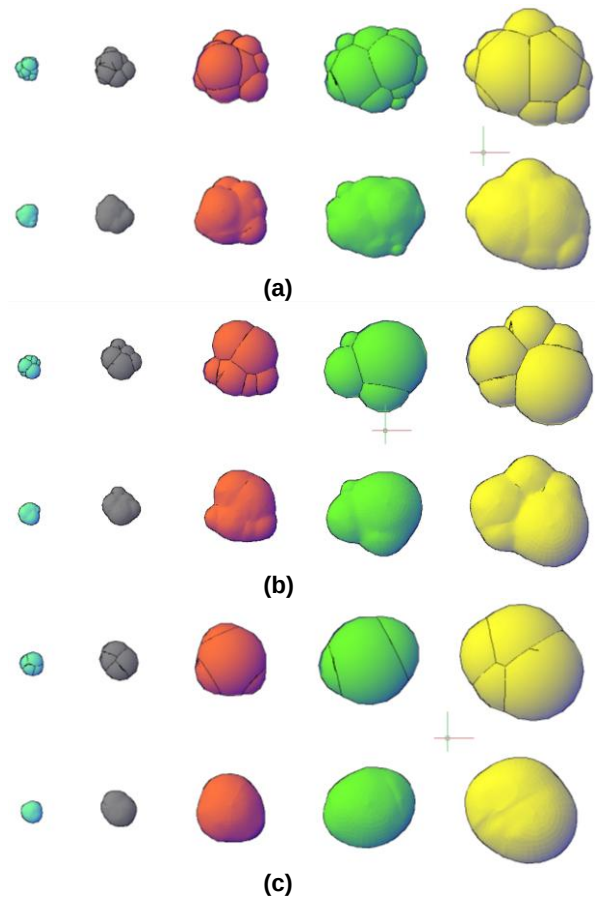


Figure 4. Assemblies generated with (a) high angular grains, (b) medium angular grains, (c) round grains

In order to have a quantitative comparison between the shapes of three series of grains two factors for every category of particles are considered as shown in table 1.

Table 1.Values of Sphericity and Angularity Index for three series of assemblies

| Particles group | Average number of spheres | Shape Description | |
|---|---|---|---|
| | | Sphericy Range,% | Ang. Index Range,% |
| High angular | 10 | 88-93 | 32-41 |
| Medium angular | 6 | 92-97 | 19-31 |
| Rounded grains | 3 | 96-99 | 7-13 |

Figure 5 shows initially generated assembly of each group with the equal porosity of about 0.69.

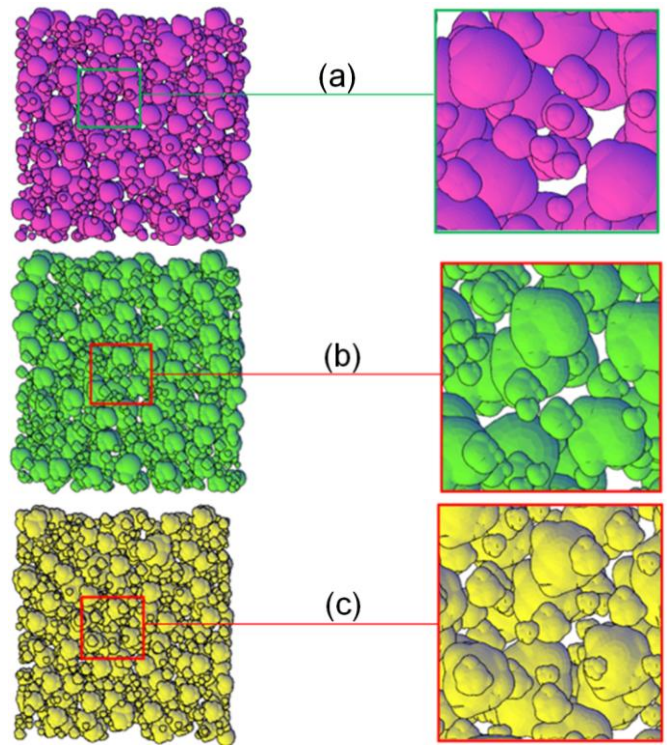


Figure 5. Initially generated assemblies, (a) Rounded grains, (b) Medium angular grains, (c) High angular grains

## 5 SIMULATED TESTS

In order to consider the effects of different factors on mechanical behaviour of granular particles, two series of tests were conducted on assemblies with different types of grains:

- Tests with different confining pressures
- Tests with different friction coefficients

In this section details of each series of tests are described

### 5.1 Tests with Different Confining Pressures

DEM parameters used in these tests are listed in Table 2. For better comparison of results, equal parameters were considered for three assemblies.

Table 2.DEM parameters used in simulated tests

| Parameters | Values |
|---|---|
| Normal contact stiffness (N/m) | $2\times10^{10}$ |
| Shear contact stiffness (N/m) | $1.3\times10^{10}$ |
| Inter-particle friction coefficient | 0.5 |
| Inter-particle cohesion | 0.0 |
| Density of particles (N/m$^3$) | $2\times10^{3}$ |
| Damping coefficient | $5\times10^{-5}$ |

The simulated tests were conducted in four stages. In the first stage, the generated assemblies were subjected

to a hydrostatic strain rate equal to $1.0\times10^{-7}$ to compact initial loose assemblies. In stage two, zero strain rates are applied in order to bring the assemblies to equilibrium. In stage three, assemblies were subjected to various isotropic confining pressures (0.15, 0.5, 1, 2 and 4 MPa). In the last stage, triaxial tests were carried out on the assemblies. In the simulated triaxial test, the horizontal stress is held constant and the vertical stress is increased by applying deviator strain rate equal to $0.5\times10^{-7}$.

### 5.2 Tests with Different Friction Coefficients

DEM parameters and their values used in these simulated tests are similar to Table 2 except for the friction coefficient that was chosen variant. The first and two stages of these tests were similar to section 6.1. In stage 3, assemblies were subjected to isotropic confining pressure equal to 1 MPa in various friction coefficients (0.1, 0.3, 0.5 and 0.7). Also, in the last stage triaxial tests were simulated with different friction coefficients and deviator strain rate equal to $0.5\times10^{-7}$.

## 6 TESTS RESULTS

The results of simulated tests are presented in two forms of charts:

- Sin of the mobilized friction angle ($\sin\phi_{mobilized}$) versus axial strain ($\varepsilon_a$)
- Volumetric strain ($\varepsilon_v$) versus axial strain ($\varepsilon_a$)

### 6.1 Test Results with Different Confining Pressures

The results of triaxial tests for assemblies with round grains in different confining pressures are shown in Figures 6 and 7. Figures 8 and 9 show the comparisons between results of triaxial tests for three series of assemblies in confining pressure equal to 2 MPa. The results for other cases are summarized in Tables 3 and 4.

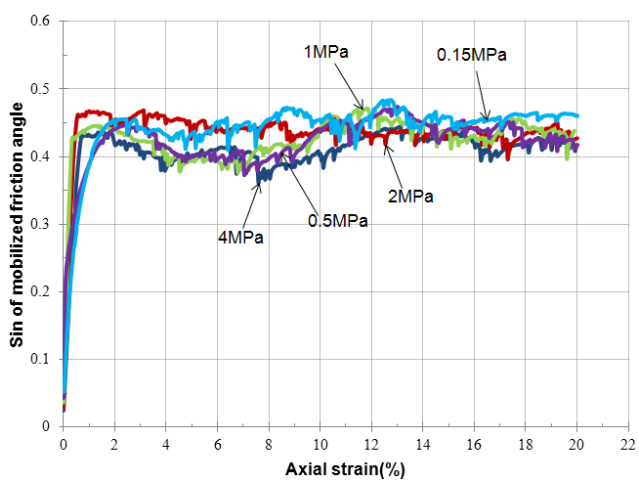


Figure 6. $\sin\phi_{mobilized}$ versus $\varepsilon_a$ for round grains in different confining pressures and $\mu$=0.5

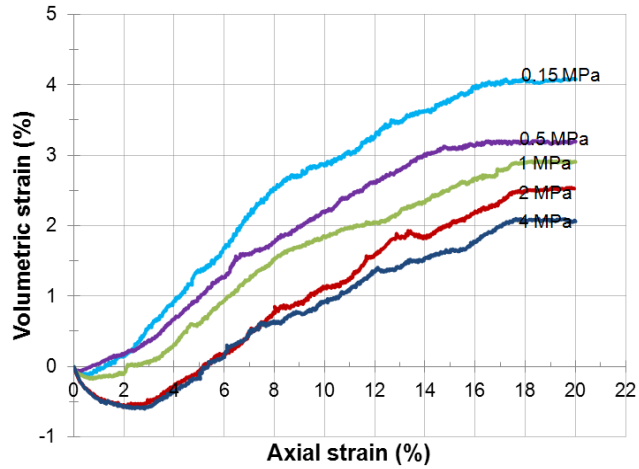


Figure 7. $\varepsilon_v$ versus $\varepsilon_a$ for round grains in different confining pressures and $\mu$=0.5

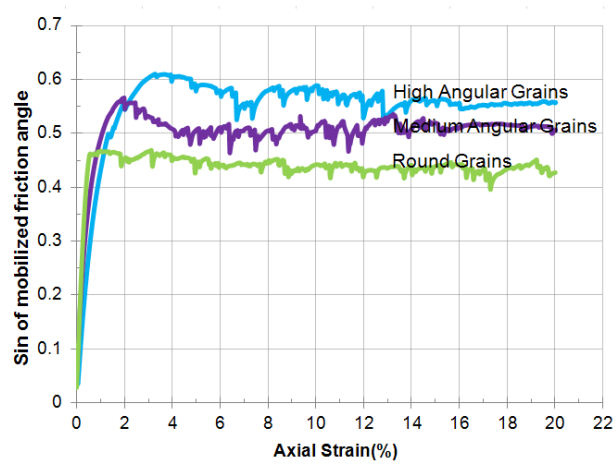


Figure 8. $\sin\phi_{mobilized}$ versus $\varepsilon_a$ for four series of assemblies in $\sigma_3$=2.0 MPa and $\mu$=0.5

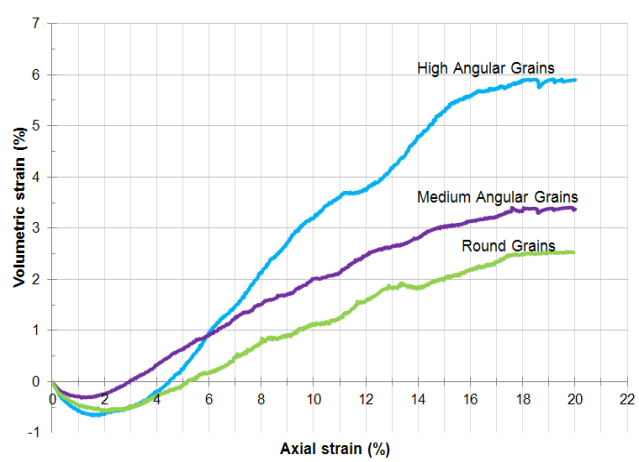


Figure 9. $\varepsilon_v$ versus $\varepsilon_a$ for four series of assemblies in $\sigma_3$=2.0 MPa and $\mu$=0.5

Table 3. $(\phi_{mobilized})_{max}$ values for three series of assemblies in different confining pressures

| Confining pressure (MPa) | $(\Phi_{mobilized})_{max}$ | | | |
|---|---|---|---|---|
| | High angular grains | Medium angular grains | Round grains | Spherical grains |
| 0.15 | 39.6° | 35.5° | 28.9° | 25.1° |
| 0.5 | 38.4° | 35.4° | 28.3° | 23.9° |
| 1 | 38.0° | 35.0° | 28.1° | 22.6° |
| 2 | 37.6° | 34.8° | 27.8° | 21.8° |
| 4 | 35.8° | 32.2° | 26.4° | 20.9° |

Table 4. Dilation values in $\varepsilon_a$=20% for three series of assemblies in different confining pressures

| Confining pressure (MPa) | Dilation value in $\varepsilon_a$=20% | | | |
|---|---|---|---|---|
| | High angular grains | Medium angular grains | Round grains | Spherical grains |
| 0.15 | 7.8% | 6.3% | 4.1% | 2.8% |
| 0.5 | 6.1% | 5.8% | 3.2% | 2.3% |
| 1 | 6.0% | 4.6% | 2.9% | 2.0% |
| 2 | 5.9% | 3.4% | 2.5% | 1.7% |
| 4 | 5.1% | 3.2% | 2.1% | 1.4% |

The following results were extracted from these figures and tables:

- The mobilized friction angle and dilation decrease with increase in confining pressure as shown in Figure 6 and Figure 7 for high angular grains; similar trend was found for other assemblies. The reason for reduction in both mobilized friction angle and dilation at higher confining pressures is that the higher confining pressures on the assembly cause to compress it more and does not let it to dilate; therefore, it doesn't allow particles to move against each other and reduction in mobilized friction angle occurs. Same conclusion can be derived for increasing minimum volumetric strain by increasing confining pressure.
- By increasing angularity the mobilized friction angle and maximum volumetric strain is increased as shown in Figure 8 and Figure 9. This increase is attributed to the interlock between particles in higher angularity. In high angular grains significant interlocking between grains exists and leads to higher shear resistance and dilation of the assembly during triaxial test.
- Numerical results of simulated tests are summarized in Tables 3 and 4. Table 3 shows the maximum of the mobilized friction angle for three series of assemblies in different confining pressures. According to this table, maximum mobilized friction angle for high angular grains in a specified confining pressure is approximately 3° to 4° greater than it for equivalent medium angular grains and 9° to 10° greater than it for equivalent round grains. Table 4 shows the values of dilation for three series of assemblies in different confining pressures in axial strain equal to 20%. According to the results, the value of dilation for high angular grains in a specified confining pressure is approximately 5% to 7% and 2% to 3% greater than its value for equivalent medium angular grains and round grains, respectively.

## 6.2 Test Results with Different Friction Coefficients

The results of triaxial tests for assemblies with high angular grains in different friction coefficients are shown in Figures 10 and 11. The results for other cases are summarized in Tables 5 and 6.

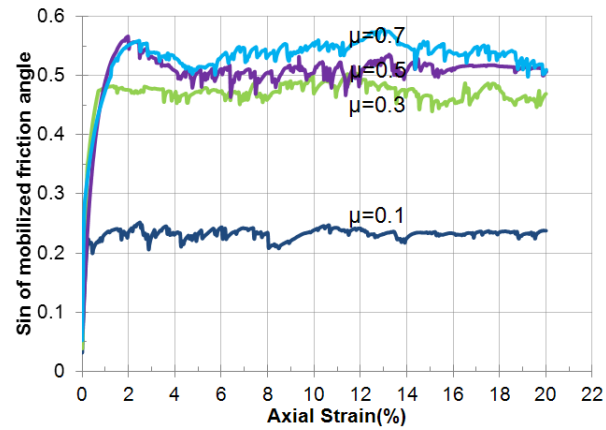


Figure 10. $\sin\phi_{mobilized}$ versus $\varepsilon_a$ for medium angular grains in different friction coefficients and $\sigma_3$=1.0MPa

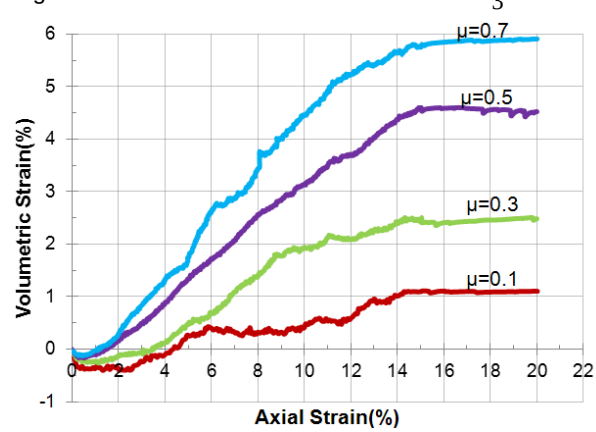


Figure 11. $\varepsilon_v$ versus $\varepsilon_a$ for medium angular grains in different friction coefficients and $\sigma_3$=1.0MPa

Table 5. $(\phi_{mobilized})_{max}$ values for three series of assemblies in different friction coefficients

| Friction coefficient (μ) | Dilation value in $\varepsilon_a$=20% | | | |
|---|---|---|---|---|
| | High angular grains | Medium angular grains | Round grains | Spherical grains |
| 0.1 | 18.3° | 14.3° | 12.9° | 12.7° |
| 0.3 | 34.6° | 30.2° | 25.4° | 21.6° |
| 0.5 | 38.0° | 35.0° | 28.1° | 22.6° |
| 0.7 | 40.2° | 35.3° | 28.9° | 25.1° |

Table 6. Dilation values in $\varepsilon_a$=18% for three series of assemblies in different friction coefficients

| Friction coefficient (μ) | Dilation value in $\varepsilon_a$=20% | | | |
|---|---|---|---|---|
| | High angular grains | Medium angular grains | Round grains | Spherical grains |
| 0.1 | 1.6% | 1.1% | 0.9% | 0.7% |
| 0.3 | 3.8% | 2.5% | 1.9% | 1.2% |
| 0.5 | 6.0% | 4.6% | 2.9% | 2.0% |
| 0.7 | 7.1% | 5.9% | 4.1% | 2.0% |

The following results were extracts from these figures and tables:

- Shear strength and dilation increase with increase in friction coefficient. It can be seen that the difference between maximum shear strength for friction coefficients equal to 0.5 and 0.7 is small and it can be deduced that the effect of friction coefficient on maximum shear strength decreases at higher values of this coefficient. As shown, with variation of friction coefficient from 0.1 to 0.3, shear strength increases significantly; it demonstrates that frictional strength constitutes considerable portion of shear strength. High angular and medium angular grains show higher increase in shear strength compare to round grains with variation of friction coefficient from 0.1 to 0.3. Moreover, the residual shear strength increases with increase in friction coefficient. Assemblies with higher friction coefficient show lower decrease in volume and higher dilation during triaxial test.
- Figure 10 and Figure 11 show that mobilized friction angle and maximum volumetric strain increase with increasing friction coefficient. These results prove that friction coefficient is a significant factor to increase the dilation and shear strength of granular materials. Friction between particles causes more strength and less displacement.
- Numerical results are summarized in Tables 5 and 6. In Table 5, maximum mobilized friction angle for three series of assemblies in different friction coefficients is shown. With increasing friction coefficient from 0.1 to 0.7, maximum of the mobilized friction angle increases $25^{\circ}$ for high angular and medium angular grains and $20^{\circ}$ for round grains. Also in a specified friction coefficient greater than zero, maximum mobilized friction coefficient for high angular grains is approximately $4^{\circ}$ to $5^{\circ}$ greater than it for medium angular grains and $9^{\circ}$ to $11^{\circ}$ greater than it for round grains. Table 6 shows the value of dilation for three series of assemblies in different friction coefficients in axial strain equal to 18%. In a case that friction coefficient was 0.1, assemblies reached to constant volume in lower axial strains; as a result, the values of dilation in this case are due to these lower axial strains. With increasing friction coefficient from 0.1 to 0.7, the value of dilation for assemblies increases approximately 5% to 8%. Also in a specified friction coefficient the value of dilation for high angular grains increases 0.5% to 2.5% and 0.5% to 3.5% compared to its value for medium angular grains and round grains, respectively.

## 7 CONCLUSION

In order to simulate the behaviour of real granular particles this paper utilizes clumping method to model angular particles with different shapes. Then by means of discrete element method a code based on centred finite-difference procedure is improved to integrate the equation of motion between particles. Three categories of grains with different angularities and sphericity consisting 1000 particles were generated and several triaxial tests with different confining pressure and friction coefficient were performed. The results can be summarized as follows:

- ✓ Mobilized friction angle and dilation improve with increase in confining pressure in a constant angularity. This increase in high angular grains is more highlighted.
- ✓ By increasing angularity in a specified confining pressure, mobilized friction angle and dilation increase significantly.
- ✓ By increasing angularity values of mobilized friction angle and dilation were increased significantly in lower confining pressure.

## 8 REFERENCES


Abou-Chakra, H., Baxter, J., Tuzun, U., 2004. Three-dimensional particle shape descriptors for computer simulation of non-spherical particulate assemblies. Advanced Powder Technology 15 (1), 63–77.

Abreu, C.R.A., Tavares, F.W., Castier, M., 2003. Influence of particle shape on the packing and on the segregation of spherocylinders via Monte Carlo simulations. Powder Technology 134, 167–180.

Aoki, R., Suzuki, M., 1971. Effect of particle shape on the flow and packing properties of non-cohesive granular materials. Powder Technology 4, 102–104.

Bagherzadeh-Khalkhali, A., Mirghasemi, A. A., Mohammadi, S. (2008). Micromechanics of breakage in sharp-edge particles using combined DEM and FEM. Particuology, No. 6 (5), 347-361.

Bagherzadeh-Khalkhali, A., Mirghasemi, A. A., (2009). Numerical and experimental direct shear tests oncoarse-grained soils. Particuology. No. 7 (1), 83-91.

Barbosa, R., and Ghaboussi, J., (1992), Discrete finite element method, Engineering Computations, Vol.9, 253-266.

Cleary, P.W., Sawley, M.L., 2002. DEM modelling of industrial granular flows: 3D case studies and the effect of particle shape on hopper discharge. Applied Mathematical Modelling 26, 89–111.

Cundall, P. A., and Strack, O. L. (1979). “A discrete numerical model for granular assemblies.” Geotechnique, 29(1), 47–65.

Gallas, J.A.C., Sokolowski, S., 1993. Grain non-sphericity effects on the angle of repose of granular material. International Journal of Modern Physics B 7 (9/10), 2037–2046.

Haff, P.K., 1993. Discrete mechanics. In: Mehta, A. (Ed.), Granular Matter. Springer, Berlin, pp. 141–160.

Hart, R., Cundall, P.A., Lemos, J., 1988. Formulation of a three-dimensional distinct element model—part 2: mechanical calculations for motion and interaction of a system composed of many polyhedral blocks. International Journal of Rock Mechanics and Mining Science & Geomechanics Abstracts 25 (3), 117–125.

Hart, R., Cundall, P.A., Lemos, J., 1988. Formulation of a three-dimensional distinct element model—part 2: mechanical calculations for motion and interaction of a system composed of many polyhedral blocks. International Journal of Rock Mechanics and Mining Science & Geomechanics Abstracts 25 (3), 117–125.

Langston, P.A., Al-Awamleh, M.A., Fraige, F.Y., Asmar, B.N., 2004. Distinct element modelling of non-spherical frictionless particle flow. Chemical Engineering Science 59, 425–435.

Lin, X., and Ng, T.T., (1997), A three-dimensional discrete element model using arrays of ellipsoids, Geotechnique, Vol. 47,No. 2,pp. 319-329.

Liu, L.X., Litster, J.D., 1991. The effect of particle shape on the spouting properties of non-spherical particles. Powder Technology 66, 59–67.

Hogue, C., 1998. Shape representation and contact detection for discrete element simulations of arbitrary geometries. Engineering Computations 15 (3), 374–390.

Hogue, C., Newland, D., 1994. Efficient computer simulation of moving granular particles. Powder Technology 78, 51–66.

Matsushima, T. and Saomto, H. 2002. Discrete element modeling for irregularly-shaped sand grains, *Proc. NUMGE2002: Numerical methods in geotechnical engineering*, Mestat (ed.), pp. 239-246

Matsushima, T., Saomoto, H., Matsumoto, M., Toda, K., and Yamada, Y. (2003). “Discrete element simulation of an assembly of irregularlyshaped grains: Quantitative comparison with experiments.” CD-ROM, 16th Engineering Mechanics Conf., Seattle.

M. Kodam, R. Bharadwaj, J. Curtis, B. Hancock, and C. Wassgren, “Force Model Considerations for Glued Sphere Discrete Element Method Simulations”, Chemical Engineering Science, 64, 3466-3475 (2009)

Mirghasemi, A.A., Rothenburg, L. and Matyas, E.L. 1997. Numerical simulations of assemblies of two-dimensional polygon-shaped particles and effects of confining pressure on shear strength, *Soils & Foundations*, 37: 43-52

Mirghasemi, A.A; Rothenburg, L. & Matyas, E. L. 2002 Influence of Particle Shape on Engineering Properties of Assemblies of Two-Dimensional Polygon-Shaped Particles*” Géotechnique,* 52, No.3, 209-217

Ng, T.T. 1994. Numerical simulation of granular soil using elliptical particles, *Computers and Geotechnics*, 16: 153-169

Nolan, G.T., Kavanagh, P.E., 1995. Random packing of non-spherical particles. Powder Technology 84, 199–205.

Ouadfel, H., Rothenburg, L., 1999. An algorithm for detecting inter-ellipsoid contacts. Computers and Geotechnics 24 (4), 245–263.

Ristow, G.H., 1994. Granular dynamics: a review of recent molecular dynamics simulations of granular materials. In: Stauffer, D. (Ed.), Annual Reviews of Computational Physics I. World Scientific, Singapore, pp. 275–308.

Rothenburg, L. and Bathurst, R.J. 1992. Micromechanical features of granular assemblies with planner elliptical particles, Geotechnique, 42: 79-95

Roberts, T.A., Beddow, J.K., 1968/69. Some effects of particle shape and size upon blinding during sieving. Powder Technology 2, 121–124.

Seyedi Hosseininia, E., Mirghasemi, A. A., (2006) Numerical Simulation of Breakage of Two-Dimensional Polygon-Shaped particles using Discrete Element Method, Powder Technology, No. 166, 100-112.

Seyedi Hosseininia, E., Mirghasemi, A. A., (2007), Effect of Particle Breakage on the Behavior of Simulated Angular Particle Assemblies, Particuology, No. 5, 328-336.

Ting, J., Khawaja, M., Meachum, L., and Rowell, J., (1993), An ellipse-based discrete element model forgranular materials, International Journal for Numerical and Analytical Methods in Geomechanics, Vol. 17,603-623.

Williams, J.R., O'Connor, R., 1995. A linear complexity intersection algorithm for discrete element simulation of arbitrary geometries. Engineering Computations 12, 185–201.

Williams, J.R., Pentland, A.P., 1992. Superquadrics and modal dynamics for discrete elements in interactive design. Engineering Computations 9, 115–127.

Xu, C., Zhu, J., 2006. Parametric study of fine particle fluidization under mechanical vibration. Powder Technology 161, 135–144.